Historical mining and smelting in the Vosges Mountains (France) recorded in two ombrotrophic peat bogs

B. Forel [a], F. Monna [a,*], C. Petit [a], O. Bruguier [b], R. Losno [c], P. Fluck [d], C. Begeot [e], H. Richard [e], V. Bichet [e], C. Chateau [f]

[a] Laboratoire ARTéHIS, UMR 5594 CNRS, Culture Université de Bourgogne, UFR SVTE, 6 bd Gabriel, F-21000 Dijon, France
[b] Géosciences Montpellier, UMR 5243 CNRS, Université Montpellier 2, CC 60, Place Eugène Bataillon, F-34095 Montpellier Cedex 5, France
[c] LISA, Universités Paris 7, Paris 12, CNRS, Faculté des Sciences, 61 av. du Gal de Gaulle F-94010 Créteil Cedex, France
[d] CRESAT, UHA, 10 rue des frères Lumière, F-68093 Mulhouse Cedex, France
[e] Laboratoire Chrono-Environnement, UMR 6249 CNRS, Université de Franche-Comté, UFR Sciences et Techniques, 16 route de Gray F-25030 Besançon Cedex, France
[f] Université de Bourgogne, UFR SVTE, 6 bd Gabriel, F-21000 Dijon, France

ARTICLE INFO

ABSTRACT

Two peat sequences were sampled in the vicinity of the main mining districts of the Vosges Mountains: Sainte-Marie-aux-Mines and Plancher-les-Mines. Lead isotopic compositions and excess lead fluxes were calculated for each of these radiocarbon-dated sequences. Geochemical records are in very good agreement with the mining history of the area, well known over the last millennium. Except for an anomaly corresponding to the Middle Bronze Age which has not yet been resolved, there is no clear geochemical evidence of local metal production in the Vosges before the 10th century as excess lead deposition archived between 500 BC and 500 AD is attributed to long-range transport of polluted particulate matter. The approach described here can be applied to other mining districts where archaeological evidence is scarce or even lacking, but where past exploitation is suspected.

© 2010 Elsevier B.V. All rights reserved.

1. Introduction

The crystalline Vosges Mountains (Northeast France) are well known for the abundant mineral resources (lead, silver, copper, and iron) they have provided through the ages. Metal production is attested from the 10th century in the district of Sainte-Marie-aux-Mines, which quickly became a rich and thriving city (Fluck, 2000). During the 15th and 16th centuries, the whole Vosges massif was intensively prospected and mined wherever possible. The locally abundant silver, which at that time was of more value than gold, was the main target. In 1545 AD, the Val d'Argent (or Silver Valley), located around Sainte-Marie-aux-Mines, counted 3000 miners, 600 mines and prospection areas, 12 smelters, and 150 km of galleries (Fluck and Weil, 1975). The history of metal production is nevertheless erratic, marked both by success stories and by declining profitability related to market competition, wars and natural catastrophes, wood supply and

other technical constraints (Fluck, 2000). The operations finally stopped in the mid-20th century after a millennium of documented activity. Many galleries, tailings and wastes are still visible in the landscape. They clearly testify to the magnitude of this rich industrial past.

The most recent periods of activity are known from field evidence (more particularly at Sainte-Marie-aux-Mines where major archaeological work has been undertaken by Fluck and colleagues), written archives, and abundant iconographic documentation (e.g. the exceptional paintings by Heinrich Groff ca. 1530 AD, reproduced in Bari et al., 1992). However, the emergence and development of mining in the region are still not fully understood. Possible pioneer works starting from Antiquity or earlier are sometime evoked but no definitive answer can be given because field evidence is lacking. Such works may have been masked or irreparably destroyed. Recently, techniques originally developed by geoscientists have been adapted to reduce these gaps in archaeological knowledge (Mighall et al., 2002, 2009; Monna et al., 2004a,b; Arnaud et al., 2004; Baron et al., 2005). The basic idea is that if mining has taken place, it will have introduced significant quantities of metals into the surrounding area. Such environmental

---

* Corresponding author. Tel.: +33 3 80 396 360; fax: +33 3 80 396 387.
E-mail address: Fabrice.Monna@u-bourgogne.fr (F. Monna).

changes are therefore able to supply indirect evidence, provided that they have been well preserved over time. Ombrotrophic peatlands may fulfil such requirements. They are almost exclusively fed by the atmosphere so that mineral matter inputs are expected to be low (Shotyk, 1996a,b) and they are supposed to be hydrologically isolated from the substratum. Finally, anthropogenic contributions can be more easily extracted from the raw geochemical signal, and hence interpreted in historical terms (Shotyk et al., 1998, 2003; Mighall et al., 2002; Kylander et al., 2005; Jouffroy-Bapicot et al., 2007; see also Bindler, 2006 for a review). Among all metals studied, lead is often the

most informative because its affinity with organic matter tends to prevent post-depositional migration (Dumontet et al., 1990; Vile et al., 1999; Shotyk et al., 1997, 2003; Weiss et al., 1999). Lead was not necessarily exploited by prehistoric societies, but because it is associated to many ore deposits including copper, it can be regarded as a proxy for various types of mining.

In the present study, we aim to establish a continuous history of metal-related activities in the Vosges massif, from the first signs of metallurgy to the most recent periods. The exceptional richness of archaeological and historical records in the region is a considerable
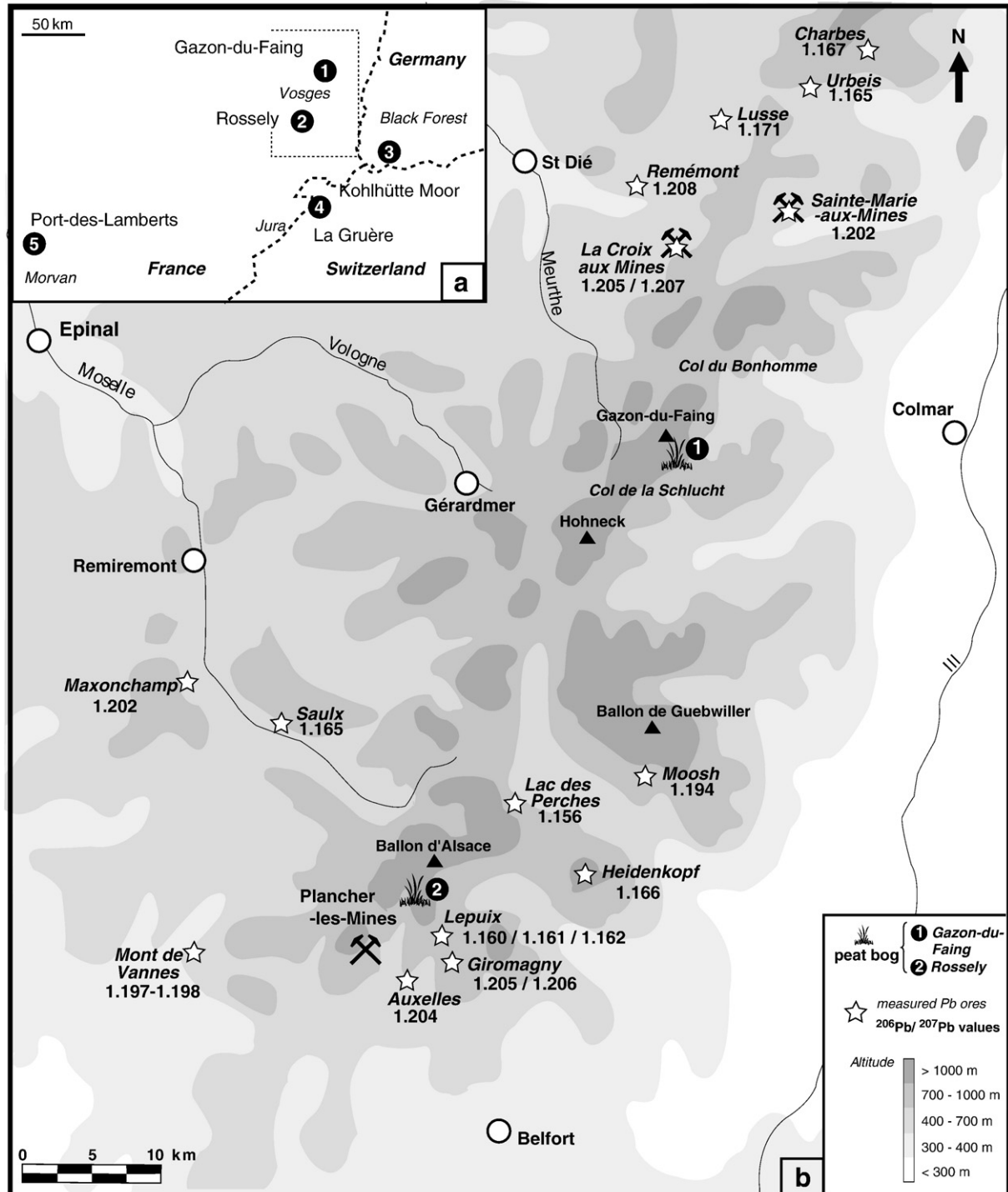

Fig. 1. (a) Geographical situation of the two sites studied, together with other peatlands previously studied (Shotyk et al., 1998; Monna et al., 2004a; Le Roux et al., 2005); (b) Map of Vosges Mountains and sampling sites. The ^{206}Pb/^{207}Pb ratios of some Pb ore deposits measured by Marcoux (1987) are also reported.

Table 1

Quality control for the analysis of the Gazon-du-Faing core performed with an ICP–MS HP-4500. Limits of detection (LOD) are calculated on the basis of 3 times the standard deviation of 4 analytical blanks. Measured and certified values of SRMs NIST 1547 and BHVO.

		Pb	Zn	Cu	La	Sr	Bi
LOD (ng g^{-1})		0.1	2	0.1	0.001	0.06	0.002
NIST 1547 (µg g^{-1})							
Measured	a	0.94	21.3	3.8	9.1	55.4	0.050
	b	0.95	22.1	3.6	8.3	50.8	0.060
Certified		0.87	17.9	3.7	9*	53	–
BHVO (µg g^{-1})							
Measured		1.95	104	130	15.3	393	0.019
Certified		2	105	136	15.2	400	0.018*

*: provided but not certified.

Table 2

Quality control for the analysis of the Rossely core performed with a VG PQ2+. Limits of detection (LOD) are calculated on the basis of 3 times the standard deviation of 4 blanks. Measured and certified values of NIST 1547.

		Pb	Zn	Cu	La	Sr
LOD (ng g^{-1})		0.1	1	0.2	0.005	0.2
NIST 1547 (µg g^{-1})						
Measured	a	1.01	22.6	3.9	8.7	56.2
	b	0.83	17.8	3.4	7.8	48.8
	c	1.20	16.0	3.8	8.7	54.8
Certified		0.87	17.9	3.7	9*	53

*: provided but not certified.

asset which allows the potentialities of this palaeoenvironmental approach to be clearly evaluated over the last millennium. The two peat bogs studied, about 80 km apart, are located near the most important Pb/Zn/Ag mining districts in the Vosges: Sainte-Marie-aux-Mines and Plancher-les-Mines. Lead isotopes were measured in addition to elemental concentrations because they have proved to be a powerful tool to discriminate natural vs. anthropogenic lead in the environment, and even to distinguish between several anthropogenic sources (e.g. Faure, 1986; MacKenzie and Pulford, 2002; Mihaljevič et al., 2006; Kylander et al., 2009; Bindler et al., 2009; see also Komárek et al., 2008 for a complete review in the environment). It has been demonstrated that two populations of galena characterised by distinct lead isotopic compositions coexist in the Vosges Mountains (Marcoux, 1987). In such conditions, the use of lead isotopic compositions should be particularly informative.

2. Materials and methods

The peat deposits of Rossely (06°48′01″E–47°49′01″N, altitude 920 m) and Gazon-du-Faing (07°03′10″E–48°05′20″N, altitude 1220 m) developed after glacial retreat (Fig. 1). They have a surface area of 10 ha and 9 ha, respectively. A Russian peat corer (5 cm in diameter and 50 cm in length) was used to collect the sequences, following a twin-core coring (10 cm of overlap). The samples were wrapped in clean plastic bags immediately after collection in order to prevent external contamination. Master series were reconstructed at the laboratory on the basis of the sampling depths. Sub-sampling of the sequences, respectively 500 and 350 cm in length, was concentrated within the topmost 300 cm in the case of Rossely, and regularly spaced for Gazon-du-Faing. The sub-samples were dried for 2 days at 60 °C and powdered with a manual agate mortar to obtain homogeneous, fine powders. Water content (WC) was calculated taking into account humid and dried sample weights. Each sample was measured two or three times by elemental analyser at the CNRS Central Laboratory (Vernaison, France) for total organic carbon (TOC) and nitrogen contents. The results were averaged and uncertainties were typically of ±5%. Loss on ignition (LOI) was performed by ashing approximately 1 g of dried peat samples at 450 °C for 4 h.

About 100 mg of peat material was first oxidized with 2 mL of HNO$_3$ of suprapure grade for 2–3 h on a hot plate. Complete digestion was then achieved under pressure on a hot plate using a mixture of 2 mL each of suprapure grade HCl, HNO$_3$ and HF (Merck, Germany). A one-third aliquot of solution was evaporated. The residues were retaken with HNO$_3$ and precisely diluted with MilliQ water. Lanthanum, strontium, and lead contents were measured using two different quadrupole-based inductively coupled plasma–mass spectrometers (ICP–MS): a HP 4500 for the Gazon-du-Faing sequence (measurements also included bismuth contents), and a VG PQ2+ for the Rossely sequence. Blanks and certified reference materials (BHVO and Peach Leaves — NIST 1547) were prepared and added to the set of unknown samples following the same protocol (Tables 1–2). The concentrations measured for standard materials were within ±10–15% of certified values. Uncertainties of ±15% were therefore considered for all elements measured by ICP–MS. Lead from the remaining two-thirds aliquot was pre-concentrated on ionic resin AG1X4 (Biorad) and measured for isotopic abundance by Q-ICP–MS. Details regarding lead separation, instrumental settings, mass bias correction by bracketing, and dead time correction can be found elsewhere (Monna et al., 1998, 2000). The BCR-1, a certified reference material processed together with peat samples, yielded lead isotopic compositions (^{206}Pb/^{207}Pb = 1.205 ± 0.004 and ^{208}Pb/^{206}Pb = 2.053 ± 0.006, at 95% confidence level) in good agreement with values reported in the literature (^{206}Pb/^{207}Pb = 1.2036 and ^{208}Pb/^{206}Pb = 2.0582; Baker et al., 2004). Blank corrections for isotopic measurements were never required because they appeared negligible compared to the total amount of lead in the aliquots. Six bulk samples for the Rossely core and five for the Gazon-du-Faing core were dated by radiocarbon (accelerator mass spectrometry) at the Poznań Radiocarbon Laboratory (Table 3). The dates were calibrated with the OxCal v.4.0 software (programme available for online use at https://c14.arch.ox.ac.uk/oxcal).

Table 3

Age–depth relationship for the cores of Rossely and Gazon-du-Faing. The data are calibrated to calendar dates AD or BC.

Site	Bulk sample	Lab. reference	Uncalibrated ^{14}C date (±1σ)	Calibrated calendar date (2σ)
Rossely	ROS 61–63	POZ-7322	740 ± 35 BP	[1220–1299] AD
	ROS 103–105	POZ-7193	1170 ± 30 BP	[778–902] AD
	ROS 153–155	POZ-7324	1605 ± 35 BP	[384–542] AD
	ROS 203–205	POZ-7194	2685 ± 30 BP	[897–802] BC
	ROS 254–256	POZ-7325	3240 ± 40 BP	[1617–1428] BC
	ROS 305–307	POZ-7195	3625 ± 35 BP	[2041–1884] BC
Gazon-du-Faing	GDF 44–45	POZ-17250	620 ± 30 BP	[1290–1400] AD
	GDF 97–98	POZ-17252	970 ± 35 BP	[990–1160] AD
	GDF 159–160	POZ-17253	1355 ± 30 BP	[620–770] AD
	GDF 224–225	POZ-17254	1845 ± 35 BP	[70–250] AD
	GDF 285–286	POZ-17255	2250 ± 35 BP	[400–200] BC

3. Results and discussion

3.1. Growing rate of the peat sequences

The age vs. depth relationship (Fig. 2) indicates fairly regular growing rates for each of the two sequences except, to some extent, for a relative slowing down between ~150 and 200 cm depth at the Rossely site. The sequences present no evident hiatus or major disturbance. The Rossely core covers more than four millennia, while the base of the Gazon-du-Faing core corresponds approximately to the transition between the Late Bronze Age and the Early Iron Age (ca. 8th century BC). Although the Gazon-du-Faing core is shorter than the Rossely core, the durations of both are adequate for our purpose.

3.2. Trophic status of the sequences

Both cores exhibit similar features with total organic carbon contents close to 50%, ash content ca 2–3% (100-LOI%), and

Fig. 2. Depth vs. ^{14}C-based calibrated calendar dates for the peat bogs of Rossely (a) and Gazon-du-Faing (b). The error bars are given with a 95% confidence level.

concentrations of lanthanum (a lithogenic, conservative element belonging to the rare earth group, used as a surrogate for mineral matter) most of the time below 1 µg g^{-1}. (Tables 4–5; Fig. 3a and b). The high C/N ratios from 20 to more than 100 (Tables 4–5) confirm the visual examination of the sequences in the field: the sequences are homogeneous, and the organic matter is not strongly decomposed, even in deep horizons. The stable water content (w/w) with depth, at about 90% for Gazon-du-Faing and Rossely (not shown here), can easily be explained by the high water retention capacity of organic matter. All these features, as well as relatively steady Sr concentrations, below 20 µg g^{-1} (Tables 4–5; Fig. 3a and b), are characteristic of ombrotrophic status (e.g. Shotyk, 2002; De Vleeschouwer et al., 2007) well adapted to our purpose.

3.3. Data preparation

Even if both sequences are ombrotrophic, metal contributions of natural origin from the atmosphere cannot be excluded. While they are obviously of minor importance in the presence of large anthropogenic inputs, they constitute the heart of the signals observed during pre-anthropogenic times. Traditionally, the isolation of the excess metal contribution (assumed to be of anthropogenic nature) with respect to natural inputs is performed in two steps. In the first step, the targeted metal is normalised to a lithogenic and conservative element such as scandium, lanthanum, or aluminium, assuming that, in natural conditions, there is a proportional relationship between buried metals of natural origin (and present at trace levels) and the element used for normalisation (e.g. Martínez-Cortizas et al., 1997, 2002; Weiss et al., 2002; Monna et al., 2006). Then the excess contribution can be computed by using the following equation:

$$M_{\text{excess}} = M_{\text{total}} - La \times (M/La)_{\text{natural}},$$

where M_{total} represents the total metal M concentration; M_{excess}, the excess contribution to the total concentration; La is the total lanthanum content, chosen here as a surrogate for natural mineral matter in this equation; $(M/La)_{\text{natural}}$ is supposed to be constant and corresponds to the ratio between the metal M and lanthanum contents in pre-anthropogenic conditions.

Fig. 4a and b presents evolutions in total Pb concentrations and Pb/La ratios and ^{206}Pb/^{207}Pb ratio profiles, for both cores. Because lanthanum contents do not vary widely with depth, the Pb/La profiles are comparable to those of total Pb. Below 300 cm depth in the Rossely core, Pb/La ratios are low and relatively steady: 2.6 ± 1.5 (1σ). Similar values are found at the base of the Gazon-du-Faing core: 2.0 ± 0.7 (1σ), although it is not certain that the background was attained. These values are about 4–5 times greater than that the typical value of the upper continental crust (Pb/La ~ 0.5, Wedepohl, 1995), but should be preferred here as reference values, because they probably depict the local geochemical background better. Excess Pb profiles, computed using a Pb/La ratio of 2.3 ± 2 (1σ), for both cores, are shown in Fig. 4a and b. For each core, they appear to be almost the same as those of total lead because the natural contribution is too low to be significant. Surprisingly, below 300 cm depth in the Rossely core, in other words in horizons formed before 2000 BC, the ^{206}Pb/^{207}Pb ratios of ~1.18 (Table 4, Fig. 4a) are markedly lower than those generally observed for Pb naturally present at trace level in rocks and soils, supposed to be between 1.19 and 1.22 in France (Elbaz-Poulichet et al., 1986; Shotyk et al., 1998; Alfonso et al., 2001; Lévêque et al., 2002). It is nonetheless worth mentioning that values of 1.18–1.19 have already been reported by Le Roux et al. (2005) for lead isotopic compositions of pre-anthropogenic horizons in a peat column collected in the Black Forest, Germany, on the other side of the Rhine. Here, this signature probably reflects the local natural atmospheric deposition, as previously suggested for the Hercynian massif of the Black Forest by Le Roux et al. (2005).
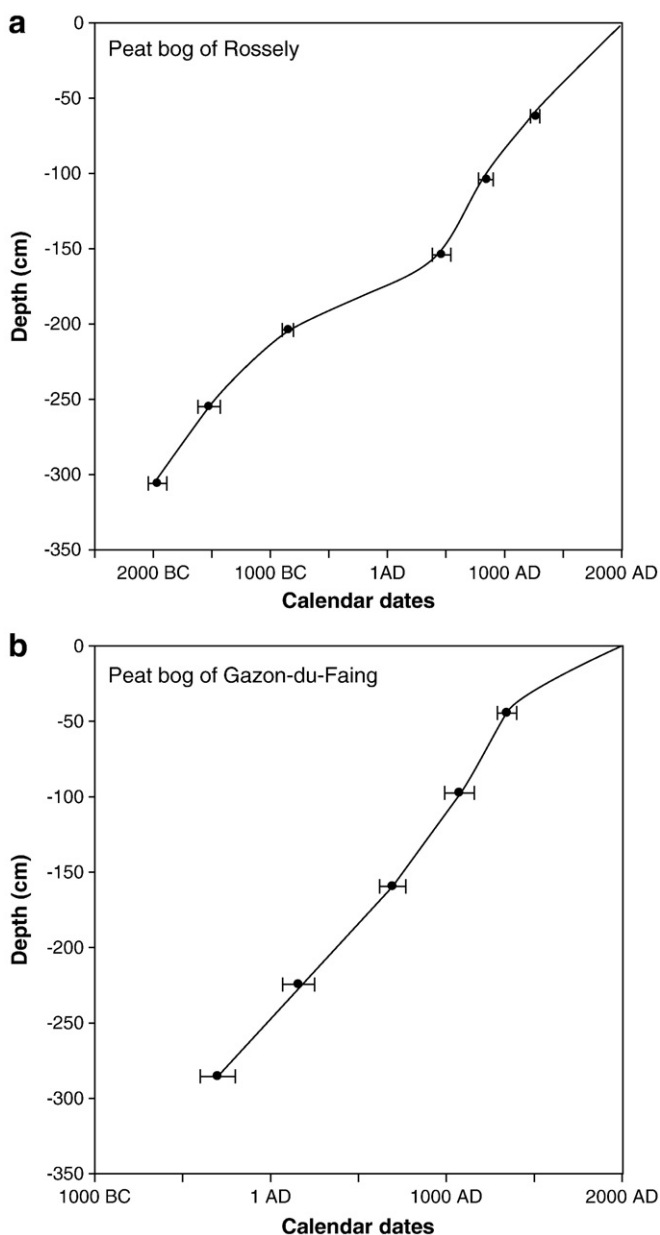
Table 4

Core of Rossely. Total organic carbon (TOC), nitrogen contents, C/N ratios, loss on ignition (LOI), La, Sr, Cu, Zn, and Pb contents and $^{206}Pb/^{207}Pb$ and $^{208}Pb/^{206}Pb$ ratios. The errors for isotopic ratios are given at 95% confidence level. See text for errors in concentration measurements.

Depth (cm)	TOC (%)	N (%)	C/N	LOI (%)	La (µg g⁻¹)	Sr (µg g⁻¹)	Pb (µg g⁻¹)	$^{206}Pb/^{207}Pb$	±	$^{208}Pb/^{206}Pb$	±
−3	47.2	2.5	19	–	2.4	24.1	278	1.166	0.005	2.085	0.009
−6	47.4	2.2	22	–	1.0	13.6	133	1.179	0.009	2.093	0.013
−12	47.9	1.4	33	96.2	0.48	13.1	415	1.198	0.010	2.064	0.015
−18	48.1	1.2	42	–	0.32	11.9	–	–	–	–	–
−20	–	–	–	–	0.60	10.6	452	1.199	0.001	2.068	0.009
−24	47.5	0.77	62	–	1.5	4.0	283	1.195	0.005	2.065	0.014
−27	46.2	0.70	66	–	0.14	5.3	283	1.195	0.008	2.063	0.021
−30	–	–	–	–	0.51	9.4	–	–	–	–	–
−33	49.8	1.6	31	–	0.43	5.5	89	–	–	–	–
−39	49.3	1.0	48	–	0.80	8.1	48	1.197	0.008	2.078	0.016
−40	–	–	–	–	0.38	5.9	84	1.198	0.002	2.063	0.005
−45	49.8	1.3	37	–	0.61	10.0	17	1.185	0.007	2.078	0.020
−55	48.6	1.0	50	–	0.40	6.9	69	1.191	0.009	2.080	0.016
−59	49.1	0.88	56	98.0	0.20	6.5	106	1.193	0.006	2.064	0.016
−67	49.5	1.3	37	–	0.22	4.7	14	1.186	0.008	2.086	0.014
−71	48.5	0.88	55	–	0.24	8.1	15	1.175	0.006	2.090	0.017
−75	48.2	0.82	59	–	0.50	3.4	4.8	–	–	–	–
−78	–	–	–	–	0.21	4.1	4.6	1.180	0.004	2.085	0.005
−83	47.2	0.79	60	98.7	0.21	7.1	6.4	–	–	–	–
−87	48.7	0.89	55	–	0.23	8.3	7.7	–	–	–	–
−91	48.1	0.67	72	–	0.10	5.2	6.0	–	–	–	–
−95	49.8	0.95	52	–	0.20	3.8	5.5	–	–	–	–
−96	–	–	–	–	0.44	5.8	3.1	1.186	0.003	2.074	0.007
−107	48.5	0.88	55	–	–	–	–	–	–	–	–
−115	–	–	–	–	0.70	7.8	3.7	1.174	0.003	2.083	0.011
−119	48.9	0.99	49	–	–	–	–	–	–	–	–
−125	48.8	0.92	53	98.9	0.50	11.8	2.4	1.174	0.004	2.087	0.009
−137	48.6	1.2	42	–	–	–	–	–	–	–	–
−143	48.8	0.97	50	–	–	–	–	–	–	–	–
−146	–	–	–	–	0.54	6.1	2.8	1.166	0.003	2.094	0.006
−147	47.9	0.93	52	–	–	–	–	–	–	–	–
−153	–	–	–	–	0.57	5.6	2.4	1.174	0.003	2.087	0.007
−155	49.0	1.1	47	98.8	–	–	–	–	–	–	–
−161	51.1	1.5	35	–	–	–	–	–	–	–	–
−167	49.6	1.4	35	–	–	–	–	–	–	–	–
−173	50.9	1.9	27	–	–	–	–	–	–	–	–
−175	–	–	–	–	0.92	6.7	10	1.178	0.003	2.092	0.007
−179	51.4	1.8	28	–	–	–	–	–	–	–	–
−185	–	–	–	–	2.1	8.0	22	1.179	0.003	2.097	0.005
−191	51.6	0.71	73	–	–	–	–	–	–	–	–
−196	–	–	–	–	0.97	6.3	8.5	1.178	0.003	2.089	0.006
−197	50.7	1.1	46	98.6	–	–	–	–	–	–	–
−203	–	–	–	–	0.72	5.6	3.0	1.179	0.004	2.089	0.004
−207	48.5	0.81	60	–	–	–	–	–	–	–	–
−219	50.3	1.3	40	–	–	–	–	–	–	–	–
−225	50.1	0.90	56	98.6	0.68	6.7	0.9	1.183	0.005	2.084	0.009
−237	48.2	0.75	64	–	–	–	–	–	–	–	–
−243	49.4	0.81	61	–	–	–	–	–	–	–	–
−245	–	–	–	–	0.49	6.3	1.1	1.179	0.008	2.078	0.016
−247	48.0	0.66	73	–	–	–	–	–	–	–	–
−253	–	–	–	–	0.76	9.5	4.9	1.159	0.002	2.098	0.006
−258	48.4	0.73	66	–	–	–	–	–	–	–	–
−265	–	–	–	–	0.46	9.7	3.1	1.162	0.003	2.095	0.005
−270	48.5	0.74	66	–	–	–	–	–	–	–	–
−276	47.9	0.52	92	–	–	–	–	–	–	–	–
−282	47.4	0.46	103	98.9	–	–	–	–	–	–	–
−285	–	–	–	–	0.40	10.3	1.8	1.169	0.005	2.089	0.012
−294	46.6	0.63	74	–	–	–	–	–	–	–	–
−295	–	–	–	–	0.38	9.9	1.6	1.165	0.006	2.096	0.013
−302	48.9	0.32	153	–	–	–	–	–	–	–	–
−303	–	–	–	–	0.41	9.9	0.6	1.183	0.002	2.086	0.005
−315	–	–	–	–	0.39	12.1	0.9	–	–	–	–
−326	47.1	0.60	79	98.8				–	–	–	–
−335	–	–	–	–	0.13	10.8	1.1	1.176	0.005	2.086	0.013
−345	–	–	–	–	0.20	11.8	1.0	–	–	–	–
−346	48.1	0.71	68	98.9	–	–	–	–	–	–	–
−360	–	–	–	–	0.20	14.0	0.4	–	–	–	–
−375	47.7	0.55	87	–	–	–	–	–	–	–	–
−389	–	–	–	–	0.15	15.8	0.7	–	–	–	–
−405	47.2	0.56	84	98.4	–	–	–	–	–	–	–
−430	–	–	–	–	0.18	20.4	0.4	–	–	–	–
−455	50.4	0.75	67	–	–	–	–	–	–	–	–
−485	–	–	–	–	0.71	6.9	0.6	1.186	0.009	2.076	0.018
−490	53.6	1.4	39	98.7	–	–	–	–	–	–	–

Table 5
Core of Gazon-du-Faing. Total organic carbon (TOC), nitrogen contents, C/N ratios, loss on ignition (LOI), La, Sr, Cu, Zn, Bi, and Pb contents and $^{206}Pb/^{207}Pb$ and $^{208}Pb/^{206}Pb$ ratios. The errors for isotopic ratios are given at 95% confidence level. See text for errors in concentration measurements.

| Depth (cm)	TOC (%)	N (%)	C/N	LOI (%)	La (μg g⁻¹)	Sr (μg g⁻¹)	Bi (μg g⁻¹)	Pb (μg g⁻¹)	$^{206}Pb/^{207}Pb$	±	$^{208}Pb/^{206}Pb$	±
−1	–	–	–	–	0.79	5.6	0.075	18	1.145	0.001	2.114	0.005
−6	–	–	–	–	1.5	4.6	0.089	37	1.130	0.001	2.128	0.004
−10	46.7	1.30	36	96.4	–	–	–	–	–	–	–	–
−15	–	–	–	–	2.1	15	0.541	158	1.165	0.002	2.096	0.005
−21	45.9	2.11	22	–	–	–	–	–	–	–	–	–
−26	–	–	–	–	1.8	7.3	0.094	46	1.184	0.002	2.080	0.006
−31	48.4	1.73	28	96.1	–	–	–	–	–	–	–	–
−36	–	–	–	–	0.79	6.9	0.027	17	1.193	0.002	2.070	0.005
−41	–	–	–	–	1.1	7.8	0.026	15	1.188	0.002	2.074	0.004
−47	–	–	–	–	1.3	11	0.037	16	1.181	0.002	2.078	0.006
−53	45.4	0.47	97	–	–	–	–	–	–	–	–	–
−58	–	–	–	–	0.53	10	0.101	18	1.181	0.002	2.083	0.006
−63	–	–	–	–	0.81	10	0.071	16	1.177	0.001	2.087	0.004
−68	46.1	0.33	140	98.3	0.65	9.8	0.045	17	1.175	0.001	2.090	0.006
−74	–	–	–	–	0.32	7.8	0.020	10	–	–	–	–
−81	–	–	–	–	0.66	11	0.021	17	1.186	0.002	2.076	0.005
−91	46.3	0.43	108	–	0.31	7.0	0.016	14	1.191	0.001	2.071	0.005
−96	–	–	–	–	0.92	9.3	0.018	14	1.190	0.002	2.070	0.004
−103	–	–	–	–	0.44	8.8	0.016	7.8	1.180	0.002	2.082	0.005
−108	44.8	0.32	140	98.7	–	–	–	–	–	–	–	–
−113	–	–	–	–	0.77	9.9	0.013	2.5	1.180	0.001	2.086	0.004
−118	–	–	–	–	0.36	6.1	0.007	1.6	1.176	0.002	2.091	0.005
−123	–	–	–	–	0.22	6.5	0.015	1.5	1.173	0.001	2.092	0.006
−129	46.3	0.20	232	–	–	–	–	–	–	–	–	–
−134	–	–	–	–	0.30	8.3	0.011	0.91	1.173	0.002	2.097	0.004
−139	–	–	–	–	0.26	8.4	0.010	1.4	1.169	0.003	2.102	0.007
−144	–	–	–	–	0.35	13	0.009	1.0	1.174	0.002	2.094	0.003
−153	46.8	0.65	72	98.6	0.61	8.0	0.018	2.4	1.177	0.002	2.086	0.004
−158	–	–	–	–	0.26	7.2	0.010	1.6	1.169	0.001	2.101	0.004
−168	44.7	0.10	447	–	0.20	7.6	0.007	0.6	1.168	0.003	2.108	0.004
−173	–	–	–	–	0.39	7.9	0.006	1.4	1.167	0.001	2.109	0.005
−178	47.0	0.27	174	99.1	0.38	8.8	0.008	0.94	–	–	–	–
−183	–	–	–	–	0.28	7.8	0.018	0.82	1.168	0.003	2.111	0.007
−188	–	–	–	–	0.47	8.5	0.016	1.6	1.172	0.002	2.096	0.002
−193	–	–	–	–	0.46	8.3	0.012	1.2	1.171	0.002	2.101	0.006
−198	47.5	0.72	66	–	0.42	6.7	0.012	1.4	1.172	0.002	2.098	0.005
−208	47.9	0.45	106	98.9	0.44	7.0	0.011	4.9	–	–	–	–
−213	–	–	–	–	0.24	5.2	0.011	7.3	1.157	0.001	2.098	0.005
−218	–	–	–	–	0.39	5.9	0.010	4.0	1.165	0.002	2.099	0.005
−223	46.3	0.19	244	99.0	–	–	–	–	–	–	–	–
−228	–	–	–	–	0.56	9.0	0.007	6.4	1.174	0.002	2.068	0.004
−238	–	–	–	–	0.53	8.7	0.016	8.0	1.171	0.002	2.095	0.005
−243	–	–	–	–	0.58	8.9	0.041	11	1.169	0.002	2.096	0.003
−248	45.8	0.30	153	98.8	0.47	9.5	0.021	8.7	1.174	0.002	2.094	0.004
−259	–	–	–	–	0.46	8.8	0.034	13	1.171	0.001	2.093	0.005
−264	46.6	0.91	51	–	–	–	–	–	–	–	–	–
−269	–	–	–	–	0.42	10	0.018	12	1.171	0.001	2.093	0.004
−274	–	–	–	–	0.36	10	0.012	9.2	1.171	0.001	2.097	0.005
−279	–	–	–	–	0.44	11	0.013	11	1.174	0.002	2.092	0.004
−284	48.1	0.25	193	98.5	0.74	10	0.025	11	1.174	0.002	2.097	0.004
−289	–	–	–	–	0.58	11	0.018	7.0	1.174	0.001	2.092	0.004
−294	48.1	0.72	67	–	0.73	11	0.025	4.6	1.178	0.001	2.093	0.005
−299	–	–	–	–	0.83	11	0.024	4.3	1.173	0.001	2.092	0.006
−308	–	–	–	–	0.57	12	0.012	1.4	1.174	0.002	2.096	0.006
−314	45.7	0.39	117	98.7	0.37	14	0.009	2.5	1.160	0.001	2.100	0.006
−320	–	–	–	–	0.28	8.6	0.008	0.76	1.174	0.002	2.097	0.004
−333	–	–	–	–	0.78	15	0.015	1.3	1.171	0.002	2.096	0.005
−339	50.5	1.53	33	98.0	0.94	12	0.020	1.4	1.177	0.002	2.097	0.006

Comparisons of excess lead profiles between cores are nonetheless difficult even when a chronological scale is preferred to a depth scale because concentrations are directly governed by growth rates of peatlands. For this reason, fluxes of excess lead were calculated for the Rossely and Gazon-du-Faing sequences by taking into account excess lead contents, accumulation rates and apparent densities (cf Mihaljevič et al. 2006). The two sequences for the Vosges are reported together with three others collected in surrounding areas (Fig. 1a, Fig. 5): (i) the "Kohlhütte Moor" sequence, located south of the Black Forest, Germany, about 90 km from our sites (Le Roux et al., 2005), (ii) the "Etang de la Gruère" sequence, in the Swiss Jura mountains, 80 km away (data in Shotyk et al., 1998, fluxes reported in Le Roux et al., 2005), and (iii) the "Port-des-Lamberts"

sequence, situated in the Morvan, Massif Central, France, 240 km away (data in Monna et al., 2004a). The $^{206}Pb/^{207}Pb$ ratios of the average anthropogenic component alone were calculated when possible using the procedure described in Monna et al. (2004a), which takes into account the $^{206}Pb/^{207}Pb$ and La/Pb ratios (or Sc/Pb ratios for the Gruère core) of both background and bulk samples.

3.4. Reading lead fluxes and lead isotopic compositions in historical terms

3.4.1. Prehistoric times–Bronze Age

Before 2000 BC, no measurable anthropogenic inputs can be recognized in the Rossely sequence (Fig. 5b). From 2000 BC to
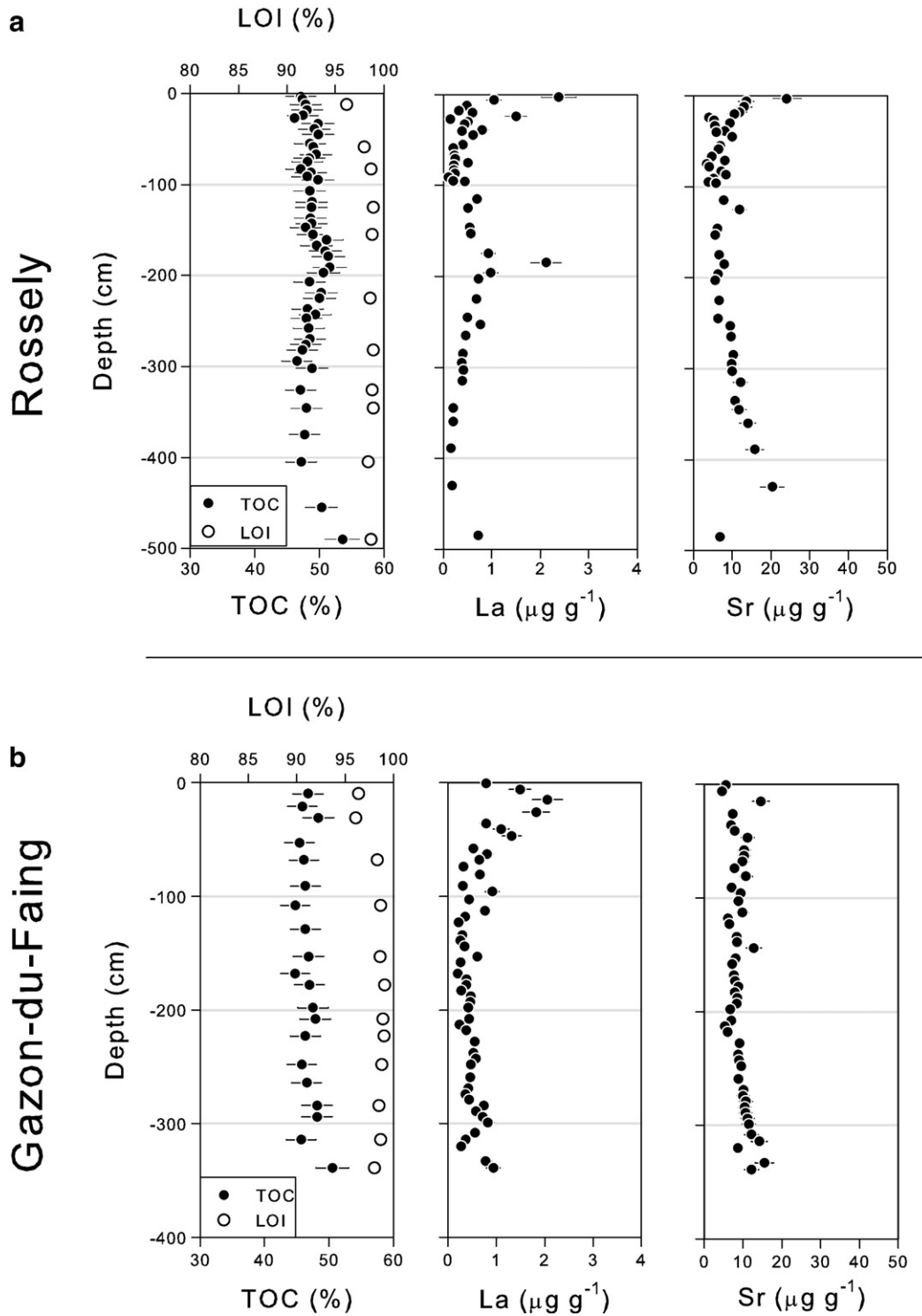
Fig. 3. Total organic carbon (TOC), loss on ignition (LOI), lanthanum, and strontium contents against depth for the cores of Rossely (a) and Gazon-du-Faing (b). The error bars are given with a 95% confidence level.

1500 BC, discrete but significant geochemical anomalies with excess Pb fluxes reaching 0.2 mg m^{-2} y^{-1} are noticed in the Rossely sequence, although nothing similar has been seen in the Morvan core, which covers the same period (Fig. 5e). This variation could perhaps be attributed to a durable episode of changes in the nature of the mineral matter integrating the peatland, in other words changes in Pb/La ratios. This hypothesis is however not fully satisfactory because the lead isotopic signature of excess lead (^{206}Pb/^{207}Pb ~ 1.155) is incompatible with natural dust inputs. Another possible explanation could be local mining by prehistoric societies, for which no archaeological evidence remains. This scenario is compatible with the lead isotopic compositions of one group of galena extracted from the surrounding ore deposits, which present ^{206}Pb/^{207}Pb ratios ~ 1.15–1.16 (see Fig. 1 for localisation and Fig. 6, details are given in Table 6). However, the available data are too scarce to confirm either hypothesis.
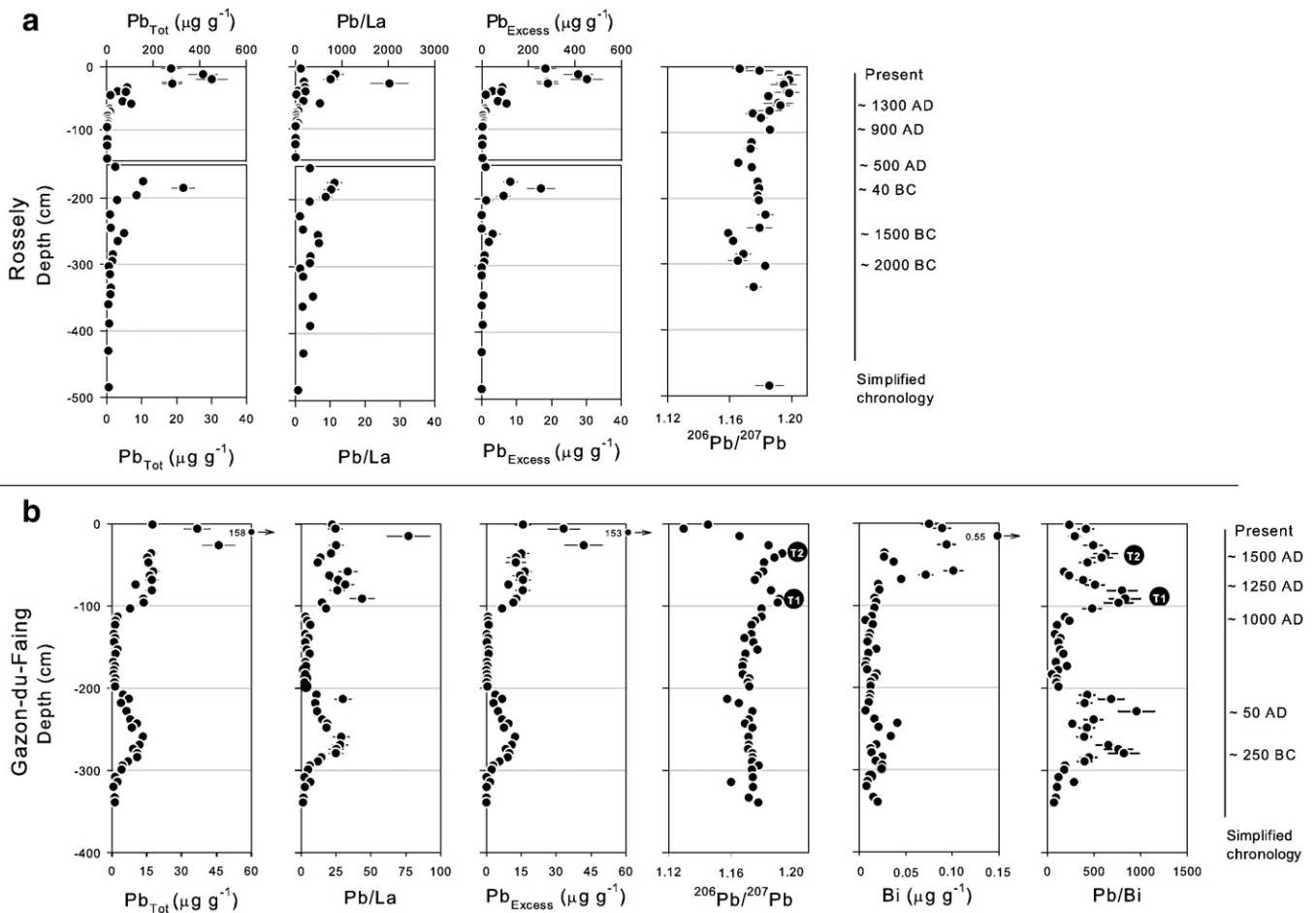
Fig. 4. Total lead, Pb/La ratios, excess lead (see text for calculation), $^{206}Pb/^{207}Pb$ ratios Bi contents, and Pb/Bi ratios against depth for the cores of Rossely (a) and Gazon-du-Faing (b). The error bars are given with a 95% confidence level.

3.4.2. Bronze Age–Antiquity

In the Rossely core, the period between 1300 BC and 600 BC is characterised by extremely low excess Pb fluxes (Fig. 5b). In contrast, the Morvan core recorded notable anthropogenic inputs during this period (Fig. 5e) which were interpreted as the impact of mining and metallurgy performed by nearby populations (Monna et al., 2004a). Significant excess Pb fluxes are noticeable in the Vosges during the Iron Age and Antiquity (Fig. 5a and b). It is well established that, during this period, mining and metallurgy developed in Europe (Settle and Patterson, 1980; Nriagu, 1983, 1996). The amount of lead introduced into the atmosphere was so large that significant fall-out of anthropogenic origin is systematically recognized in lake sediments and peat bogs across Europe (e.g. Shotyk et al., 1998; Kylander et al., 2009) reaching areas as remote as Sweden or Greenland where metallurgy was obviously not present at that time (Hong et al., 1994; Rosman et al., 1997; Brännvall et al., 1999). Because the contamination was widespread, some authors have even proposed using the lead anomaly as a chronostratigraphic marker to date sediments (Renberg et al., 2001). It is therefore not surprising to observe this signal in the Vosges Mountains. The point is nonetheless to determine if lead emitted by possible local mining may have been added in substantial amounts to that resulting from long-range transport of polluted airborne particulate matter. Comparing lead isotopic signatures of anthropogenic lead contribution and fluxes recorded in the Vosges Mountains with other neighbouring sites can help to answer this question. First of all, the anthropogenic lead flux peaked at approximately the same time in the Vosges, Morvan, Black Forest and Swiss Jura. Time shifts can be observed

between the profiles but they may be due to uncertainties in the chronology, more particularly at Rossely where the time scale is poorly constrained between 1000 BC and 1000 AD. In addition, moderate post-deposition migrations of Pb may have led to an overestimation of the contamination phase duration. There is a remarkable similarity in the maximum anthropogenic lead fluxes: about 1 mg m^{-2} y^{-1} at each of these sites, although metallic deposition is known to be controlled by local climatic and geomorphological conditions (rainfall amount, topography, etc.). However, while the isotopic signatures of the anthropogenic component were approximately the same at Rossely ($^{206}Pb/^{207}Pb \sim 1.178$–1.179, Fig. 5b), Gazon-du-Faing ($^{206}Pb/^{207}Pb \sim 1.174$–1.175; Fig. 5a) and in the Jura ($^{206}Pb/^{207}Pb \sim 1.176$–1.177; Fig. 5d), a slightly less radiogenic component was noticed in the Morvan during this period ($^{206}Pb/^{207}Pb \sim 1.170$–1.172, Fig. 5e); no isotopic data is available for the Black Forest core during Antiquity (Fig. 5c). These features plead in favour of a common remote source impacting all sites in approximately the same way. The only difference resides in the situation of the Morvan where the adjunction of locally derived pollution may have produced a mean anthropogenic component slightly less radiogenic than those calculated for the other sites. Everything therefore tends to demonstrate that, despite the abundance of mineral resources, significant local mining did not take place in the Vosges at this period.

3.4.3. Middle Ages–Modern times

Excess lead appears to be low in all cores including those from the Vosges from the 4th century AD and for six centuries onwards (Fig. 5).
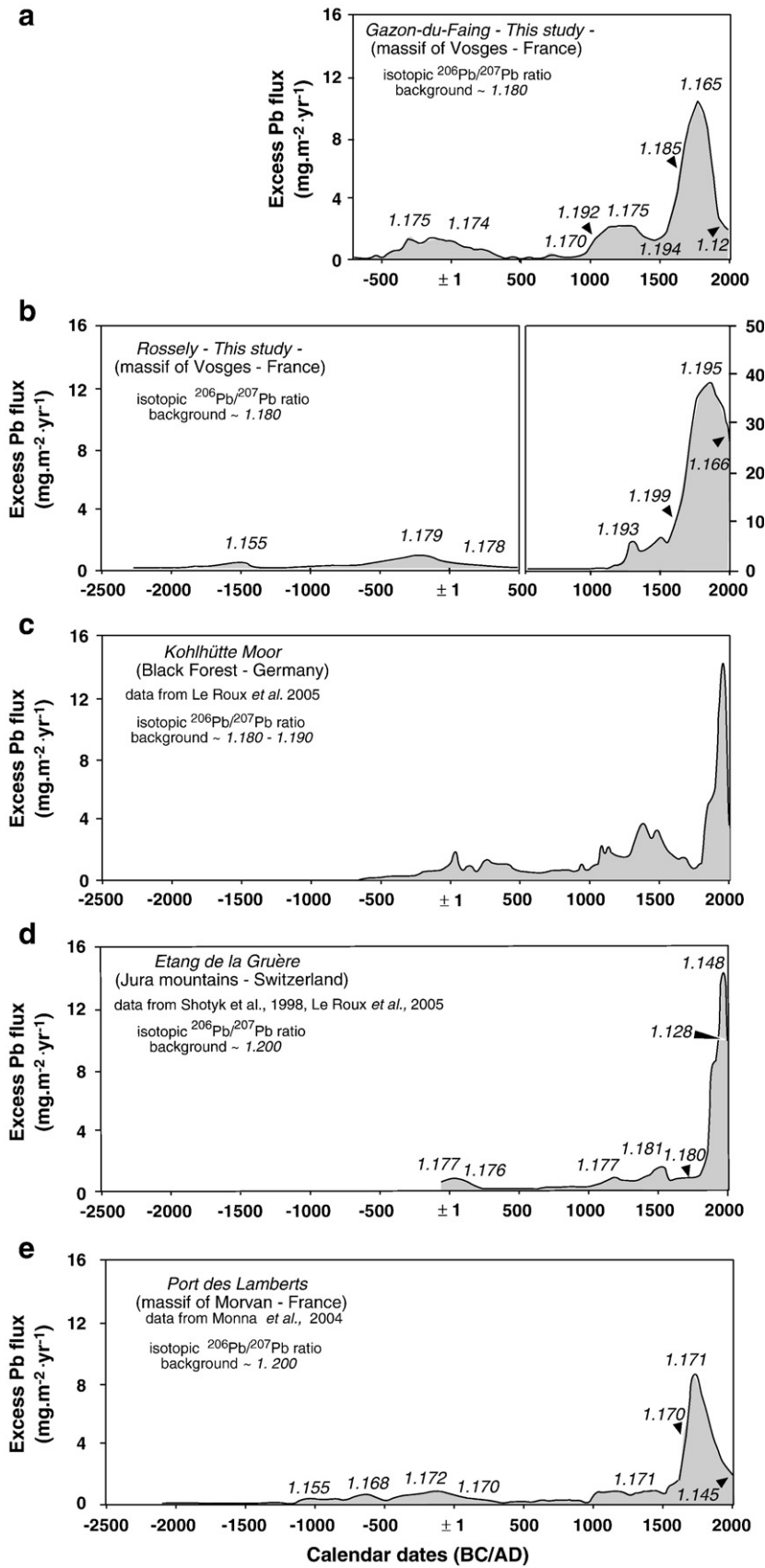
Fig. 5. Excess lead fluxes through time: Gazon-du-Faing (a) and Rossely (b) in the Vosges Moutains; Kohlhütte Moor (c) in the Black Forest; Etang de la Gruère (d) in the Swiss Jura Mountains; Port des Lamberts (e) in the Morvan massif. The isotopic [206]Pb/[207]Pb ratios of excess lead are reported on the graphs. Attention must be paid to the Rossely diagram which presents a double Y-axis scale.
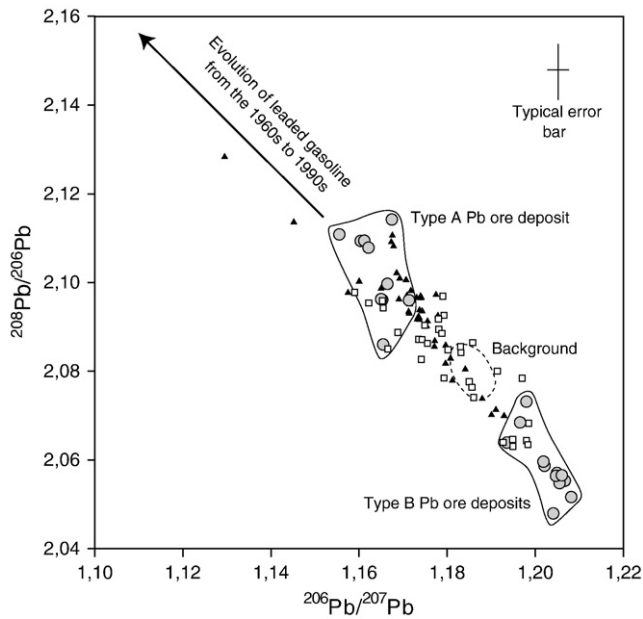
Fig. 6. $^{206}Pb/^{207}Pb$ vs. $^{208}Pb/^{206}Pb$ diagram. Open boxes and closed triangles correspond to samples from Rossely and Gazon-du-Faing respectively. Potential lead sources are reported for comparative purposes: Grey circles for local Pb ore deposits of types A and B (data from Marcoux, 1987), and recent evolution of leaded gasoline (see text for details). Typical error bars for isotopic measurements are also reported (95% confidence level).

With the fall of the Roman Empire, a period known as the Dark Ages began. Many mines closed across Europe and the main metallurgical centres slowed down. Wars and barbarian invasions disorganized industrial production and airborne particulate matter became rapidly less contaminated at the European scale (Shotyk et al., 1998; Brännvall et al., 1999). From the 10th century to the present, both environmental records and the local history of mining and smelting differ somewhat for the districts of Sainte-Marie-aux-Mines and Plancher-les-Mines. As a consequence, they are discussed separately.

3.4.3.1. Gazon-du-Faing. A drastic increase in excess Pb deposition is noticed from the 10th century (Fig. 5a). This intensification is accompanied by a major shift in lead isotopic compositions towards more radiogenic values; the calculated $^{206}Pb/^{207}Pb$ ratios of excess lead progress rapidly from 1.170 to 1.192. The oldest field evidence of mining ever found at Sainte-Marie-aux-Mines dates from that period. It is based on two radiocarbon analyses of coals (845–980 AD and 895–1015 AD) associated with scoria and furnace fragments (Fluck, 2000). Such dates are in very good agreement with the earliest written source which reports that the monk who founded the monastery of Echery (ca. 938 AD) also started mining activities in the area (Fluck, 2000 and sources cited therein). Moreover, the rise of the $^{206}Pb/^{207}Pb$ ratios toward radiogenic values is coherent with the signatures of one group of local galena, namely type B, which present $^{206}Pb/^{207}Pb$ ratios of about 1.20 (see Fig. 1 for localisation and Fig. 6, details are given in Table 6). Lead isotopic compositions of peat undoubtedly record the environmental impact of local mining and smelting. From the 11th to the 13th centuries AD, excess lead fluxes stabilised, reaching more than 2 mg m^{-2} y^{-1}, while $^{206}Pb/^{207}Pb$ ratios of the anthropogenic lead signature regularly decreased to 1.175. Smelters, galleries and hydrological installations built to wash ores, which all testify to persistent metallurgical activity from the 10th to 14th century AD have been discovered by Fluck and colleagues in the Altenberg (Sainte-Marie-aux-Mines district). The fall of the $^{206}Pb/^{207}Pb$ ratios observed in the Gazon-du-Faing peat bog probably illustrates the progressive extension of

mining works to another group of local ore deposits (i.e. galena of type A, characterised by $^{206}Pb/^{207}Pb$ ratios of about 1.165, cf Table 6, Fig. 6). There is a turning point around the 13th–14th century. Lead pollution decreased and $^{206}Pb/^{207}Pb$ ratios of the pollutant end-member rose again to values greater than 1.190 (Fig. 5a). It is known that mining declined at that time without totally collapsing (Fluck, 2009) in part because of the disorganisation of the society due to successive famines (1292–1295 and 1315–1317), the Black Plague which was particularly severe in 1348, 1359, 1370 and 1400 in the Vosges, and the Hundred Years' War lasting from 1337 to 1453. Other reasons, such as technical problems related to the accumulation of water in galleries, have also been invoked to explain this recession. Production is known to have focused only on specific mines selected for their profitability. Such a change is illustrated by the sudden shift in $^{206}Pb/^{207}Pb$ ratios toward more radiogenic values. From the beginning of the 16th century, anthropogenic lead fluxes quickly increased to reach more than 10 mg m^{-2} y^{-1} during the 17th–18th century, while $^{206}Pb/^{207}Pb$ ratios of the anthropogenic contribution dropped to 1.165 (Fig. 5a). This new turning point is in perfect agreement with the revival of mining exploitation which occurred from the end of the 15th century AD at Sainte-Marie-aux-Mines. The first success recorded from the beginning of the 16th century AD led to intense and systematic prospection. However, difficulties quickly appeared: (i) forest clearances had to extend to respond to the increasing demand for shoring beams and the wood supply decreased so that its price rose, (ii) too much silver persisted in copper ingots reducing profits, and (iii) mined veins deepened and consequently the exploitation cost increased.

Table 6
Lead isotopic compositions of Vosges ore deposits measured by TIMS (data from Marcoux, 1987). Errors were typically ±0.01, ±0.01 and ±0.02 for $^{206}Pb/^{204}Pb$, $^{207}Pb/^{204}Pb$, $^{208}Pb/^{204}Pb$ ratios, respectively (at 95% confidence level). Ak, G, Bl, Z, P, Bert., for aikinite, galena, boulangerite, zinkenite, plagionite, and berthierite. Two groups can be recognized. The less radiogenic, namely Type A, (model ages of 300–400 Ma, $^{206}Pb/^{207}Pb$ ~1.15–1.16) corresponds to high temperature deposits (Lac des Perches, Saulx), the vein of Heidenkopf, and the Pb/Sb veins (Lepuix Gy, Urbeis), while the more radiogenic includes all of the F/Ba and Ag/Pb veins, except Lusse. This group, namely Type B, is characterised by model ages from +30 Ma to −140 Ma and $^{206}Pb/^{207}Pb$ ratios of about 1.19–1.20.

Location	Mineral	$^{206}Pb/$ ^{204}Pb	$^{207}Pb/$ ^{204}Pb	$^{208}Pb/$ ^{204}Pb	$^{206}Pb/$ ^{207}Pb	$^{208}Pb/$ ^{206}Pb
High temperature ore deposits						
Lac des Perches	Ak	17.964	15.546	37.918	1.156	2.111
Saulx	G	18.120	15.547	37.798	1.165	2.086
Sainte-Marie-aux-Mines	G	18.789	15.630	38.679	1.202	2.059
Mesothermal deposits						
La Croix aux-Mines	G	18.871	15.638	38.785	1.207	2.055
La Croix aux-Mines	G	18.848	15.642	38.770	1.205	2.057
Remémont	G	18.883	15.629	38.740	1.208	2.052
Lusse	G	18.320	15.640	38.398	1.171	2.096
Urbéis	G	18.182	15.603	38.110	1.165	2.096
Urbéis	Bl	18.171	15.597	38.090	1.165	2.096
Moosch	G	18.625	15.604	38.439	1.194	2.064
Lepuix-Gy	Z	18.066	15.569	38.107	1.160	2.109
Lepuix-Gy	P	18.080	15.570	38.137	1.161	2.109
Lepuix-Gy	Bl	18.089	15.565	38.128	1.162	2.108
Charbes	Bert.	18.370	15.735	38.837	1.167	2.114
Epithermal veins						
Giromagny	G	18.869	15.652	38.770	1.206	2.055
Giromagny	G	18.844	15.642	38.750	1.205	2.056
Trémeures	G	18.877	15.652	38.820	1.206	2.056
Maxonchamp	G	18.788	15.632	38.695	1.202	2.060
Auxelles	G	18.814	15.625	38.529	1.204	2.048
Mont-de-Vannes	G	18.761	15.679	38.805	1.197	2.068
Mont-de-Vannes	G	18.787	15.682	38.947	1.198	2.073
Heidenkopf	G	18.169	15.576	38.148	1.166	2.100

Fortunately, the discovery in 1549 of a silver-rich copper vein some kilometers south of Sainte-Marie-aux-Mines in the Neuenberg (the new mountain) by Schwartz Collin strongly stimulated production. Simultaneously, a new process, liquation, which consists in adding considerable amounts of lead to copper in order to increase silver extraction, was massively applied thus improving profitability. Nonetheless, after a thirty-year period of wealth, mining declined again due to wood shortages, augmentation of production costs, and the discovery of mines in the New World which provided silver for Europe. The Thirty Years' War during the first half of the 17th century led to plundering and occupation by Swedish, French and Imperial troops. Water rose in shafts and production collapsed again. At the beginning of the 18th century, mines reopened focusing on silver, lead, copper and a newly exploited metal: cobalt. However, infrastructures suffered from fires, floods and various accidents which damaged the fragile industrial balance. A new phase of recession occurred from the second half of the 18th century. This historical summary shows that local mining and smelting underwent several peaks and troughs during the 16th–18th century. Unfortunately, they are not all visible in our profile, except the revival in the 18th century which probably corresponds to lead fluxes peaking at about 11 mg m^{-2} y^{-1} (Fig. 5a). A higher resolution sub-sampling and the establishment of a ^{210}Pb chronology over the last century, extrapolated to depth, should improve the reconstruction of this past history. However, it must be kept in mind that, because they are formed from living plants, peat sequences are probably less efficient than laminated and undisturbed sediments at preserving high-frequency variations. In all cases, the slow industrial decline of the area, which was marked only by some attempts at exploitation during the 19th century, lingering on until World War II, explains the decrease in excess lead fluxes during the 19th and 20th centuries. The low ^{206}Pb/^{207}Pb ratio ca 1.12 in the sub-surface horizon of Gazon-du-Faing (Fig. 5a) is clearly incompatible with local or regional mining (Fig. 6). In contrast, it illustrates the influence of unradiogenic lead added as an antiknock compound in gasoline from the end of the 20th century (Hamester et al., 1994; Monna et al., 1997; Chiaradia and Cupelin, 2000).

3.4.3.2. Rossely. The first signs of medieval contamination appear from the 12th–13th century in the Rossely core (Fig. 5b), in other words later than for Gazon-du-Faing. Although the medieval mining history is not well known in the district of Plancher-les-Mines, some sources seem to indicate that mining started in the area as early as the 12th century AD. The first written evidence dates from the 15th century, when the priests of Lure signed a lease for local metal exploitation. Later, during the 16th century, anthropogenic lead fluxes increased rapidly. At the beginning of the 16th century, the silver mines of Plancher-les-Mines were among the most productive in the Empire. The district furnished Guebwiller (Alsace, France) with silver for coinage. As in the case of the Sainte-Marie-aux-Mines district, the Thirty Years' War damaged local mining and smelting. Extraction and treatment works began again from the end of the 17th century, peaked during the 18th century and finally ceased in 1770. In the Rossely core, just as in the Gazon-du-Faing core, the peak of activity is clearly recorded (Fig. 5b), as is perhaps the slowing down which occurred during the first half of the 16th century. Except for the topmost samples which are less radiogenic, probably because of the influence of unradiogenic leaded gasoline, the lead isotopic compositions of the anthropogenic inputs remained steady at Rossely from the end of the 13th century to modern times, with ^{206}Pb/^{207}Pb ratios between 1.19 and 1.20 (Fig. 5b). These signatures suggest a mixture between the two types of galena recognized in the area: ^{206}Pb/^{207}Pb = 1.155–1.165 and ^{206}Pb/^{207}Pb = 1.194–1.204 (see Fig. 1 for localisation and Fig. 6, details are given in Table 6), with however a paramount importance of the second end-member. Interestingly, the isotopic differences observed between the two cores from the 10th century onwards (Fig. 5a and b) confirm that atmospheric deposition at this period is mainly driven by local mining and smelting, rather

than by inputs originating from remote sources. It is also noteworthy that excess lead fluxes appear to be much greater in magnitude at Rossely than at Gazon-du-Faing (Fig. 5a and b). It would nonetheless be false to conclude that exploitation at Plancher-les-Mines was more intense than at Sainte-Marie-aux-Mines. The peatland of Rossely is located leeward, at only 5–10 km from the main mines, while the Gazon-du-Faing peat was cored more than 20 km south of Sainte-Marie-aux-Mines (Fig. 1). Their situations with respect to supposed contamination sources are thus quite different in terms of distance from emissions and position with respect to dominant wind direction.

3.5. Bismuth as possible proxy of metallurgy

Bismuth is a metal that was often mistaken for lead in the past as they are chemically close. It may be associated as a by-product to some lead or copper ores, so that discrete but significant contamination has been observed as early as Greek/Phoenician times in Arctic ice (Krachler et al., 2009). In our case, from the medieval period and onwards, the Bi profile in the Gazon-du-Faing core exhibits some resemblance with Pb, except that it begins to increase later and that it drops appreciably during the 14th century (Fig. 4b). The resulting large variations in Pb/Bi ratios between 100 and 850 appear to be smooth and closely related to those of ^{206}Pb/^{207}Pb ratios from the Middle Ages (see the simultaneous peaks at times T1 and T2 in Fig. 4b). This similitude strongly suggests that Pb/Bi ratios might help in identifying the mineralizations exploited throughout history. As a matter of fact, the drastic rise in Bi contents from the 16th century AD onwards clearly matches mining works undertaken from 1549 in the Neuenberg, an area known to present substantial traces of Bi, while ores from Altenberg exploited earlier do not contain as much. During the Iron Age and Antiquity, high Pb/Bi ratios are also detected (Fig. 4b). They present two top values corresponding to horizons dated at approximately 250 BC and 50 AD. This feature, if it is confirmed, might be used in the future to trace the pollution deriving from long-range transport of contaminated particles across Europe.

4. Conclusion

The geochemical reading of lead signals archived in both cores is in very good agreement with the local archaeological and historical knowledge available for the two mining districts over the last millennium. This result clearly demonstrates the effectiveness of our approach. Even if the temporal resolution may appear rather poor to archaeologists and historians, it allows a rapid overview of local mining and smelting. Concerning the earliest periods, no mining or smelting was clearly identified before the 10th century. Geochemical anomalies recognized for the Iron Age and Antiquity were attributed to continental signals observed everywhere in Europe at those periods. A discrete anomaly was also noticed for the Bronze Age at the site of Rossely but its origin is not clear enough to identify local mining with confidence.

The present work also stresses the massive metal contamination in areas nowadays protected by the French government because of their remarkable biotopes. Pb concentrations reach respectively more than 100 μg g^{-1} and 500 μg g^{-1} in the sub-surface horizons of Gazon-du-Faing and Rossely. These areas are located several kilometers away from former emission sources, so that the immediate surroundings of the former mines and smelters are in all probability much more heavily contaminated. Environmental studies should therefore be undertaken to assess the impact on present-day fauna and human health.

directed by Jean-François Piningre, which studies the Bronze Age in eastern France. We are grateful to anonymous reviewers who improved the manuscript by their judicious comments.

References

Alfonso, S., Grousset, F., Massé, L., Tastet, J.-P., 2001. A European lead isotope signal recorded from 6000 to 300 years BP in coastal marshes (SW France). Atmospheric Environment 35, 3595–3605.

Arnaud, F., Revel-Rolland, M., Bosch, D., Winiarski, T., Desmet, M., Tribovillard, N., Givelet, N., 2004. A 300 year history of lead contamination in northern French Alps reconstructed from distant lake sediment records. Journal of Environmental Monitoring 6, 448–456.

Baker, J., Peate, D., Waight, T., Meyzen, C., 2004. Pb isotopic analysis of standards and samples using a Pb-207–Pb-204 double spike and thallium to correct for mass bias with a double-focusing MC–ICP–MS. Chemical Geology 211, 275–303.

Bari, H., Benoit, P., Brugerolles, E., Fluck, P., Schoen, H., 1992. La mine mode d'emploi. La Rouge Myne de Sainct Nicolas de La Croix. Collection Découvertes Gallimard. 84 pp.

Baron, S., Lavoie, M., Ploquin, A., Carignan, J., Pulido, M., de Beaulieu, J.-L., 2005. Record of metal workshops in peat deposits: history and environmental impact on the Mont Lozère Massif, France. Environmental Science and Technology 39, 5131–5140.

Bindler, R., 2006. Mired in the past — looking to the future: geochemistry of peat and the analysis of past environmental changes. Global and Planetary Change 53, 209–221.

Bindler, R., Renberg, I., Rydberg, J., Andren, T., 2009. Widespread waterborne pollution in central Swedish lakes and the Baltic Sea from pre-industrial mining and metallurgy. Environmental Pollution 157, 2132–2141.

Brännvall, M.-L., Bindler, R., Renberg, I., Emteryd, O., Bartnicki, J., Billström, K., 1999. The medieval metal industry was the cradle of modern large-scale atmospheric lead pollution in Northern Europe. Environmental Science and Technology 33, 4391–4395.

Chiaradia, M., Cupelin, F., 2000. Behaviour of airborne lead and temporal variations of its source effects in Geneva (Switzerland): comparison of anthropogenic versus natural processes. Atmospheric Environment 34, 959–971.

De Vleeschouwer, F., Gerard, L., Goormaghtigh, C., Mattielli, N., Le Roux, G., Fagel, N., 2007. Atmospheric lead and heavy metal pollution records from a Belgian peat bog spanning the last two millennia: human impact on a regional to global scale. Science of the Total Environment 377, 282–295.

Dumontet, S., Lévesque, M., Mathur, S.P., 1990. Limited downward migration of pollutant metals (Cu, Z, Ni, and Pb) in acidic virgin peat soils near a smelter. Water Air Soil Pollution 49, 329–342.

Elbaz-Poulichet, F., Holliger, P., Martin, J.M., Petit, D., 1986. Stable lead isotopes ratios in major french rivers and estuaries. Science of the Total Environment 54, 61–76.

Faure, G., 1986. Principles of Isotope Geology. Wiley and sons, NewYork, USA.

Fluck, P., 2000. Sainte-Marie-aux-Mines. Les mines du rêve. Editions du patrimoine minier, p. 208.

Fluck, P., 2009. PCR Altenberg (Ste-Marie-aux-Mines, Haut-Rhin): fonderies et mines d'argent, Xe-XVIIe s., Les Actes du CRESAT, No. 6. Université de Haute-Alsace.

Fluck, P., Weil, R., 1975. Géologie des gîtes minéraux dans les Vosges: Mémoires du B.R. G.M., 87, p. 190.

Hamester, M., Stechmann, M., Steiger, M., Dannecker, W., 1994. The origin of lead in urban aerosols — a lead isotopic ratio study. Science of the Total Environment 146/147, 321–323.

Hong, S., Candelone, J.P., Patterson, C.C., Boutron, C.F., 1994. Greenland ice evidence of hemispheric lead pollution two millenia ago by Greek and Roman civilizations. Science 265, 1841–1843.

Jouffroy-Bapicot, I., Pulido, M., Galop, D., Monna, F., Ploquin, A., Baron, S., Petit, C., Lavoie, M., Beaulieu, J.-L., de Richard, H., 2007. Environmental impact of early palaeometallurgy: pollen and geochemical analysis. Vegetation History and Archaeobotany 16, 251–258.

Komárek, M., Ettler, V., Chrastný, C., Mihaljevič, M., 2008. Lead isotopes in environmental sciences: a review. Environment International 34, 562–577.

Krachler, M., Zheng, J., Fisher, D., Shotyk, W., 2009. Global atmospheric As and Bi contamination preserved in 3000 year old Arctic ice. Global Biogeochemical cycles 23, GB3011 7 pp..

Kylander, M.E., Weiss, D.J., Martínez Cortízas, A., Spiro, B., Garcia-Sanchez, R., Coles, B.J., 2005. Refining the pre-industrial atmospheric Pb isotope evolution curve in Europe using an 8000 year old peat core from NW Spain. Earth and Planetary Science Letters 240, 467–485.

Kylander, M.E., Weiss, D.J., Kober, B., 2009. Two high resolution terrestrial records of atmospheric Pb deposition from New Brunswick, Canada, and Loch Laxford, Scotland. Science of Total Environment 407, 1644–1657.

Le Roux, G., Aubert, D., Stille, P., Krachler, M., Kober, B., Cheburkin, A., Bonani, G., Shotyk, W., 2005. Recent atmospheric Pb deposition at a rural site in southern Germany assessed using a peat core and snowpack, and comparison with other archives. Atmospheric Environment 39, 6790–6801.

Lévêque, J., Phillippe, S., Baize, D., Monna, F., Haack, U., 2002. Utilisation des isotopes stables du plomb pour la détermination des sources de pollutions et l'étude de son transfert dans les sols contaminés. In: Baize, D., Tercé, M. (Eds.), « Les éléments traces métalliques dans les sols. Approches fonctionnelles et spatiales » INRA: coord., pp. 341–391.

MacKenzie, A.B., Pulford, I.D., 2002. Investigation of metal dispersal from a disused mine site at Tyndrum, Scotland, using concentration gradients and stable Pb isotope ratios. Applied Geochemistry 17, 1093–1103.

Marcoux, E., 1987. Isotopes du plomb et paragenèses métalliques. Traceurs de l'histoire des gîtes minéraux. Document du BRGM, No. 117. 289 pp.

Martínez-Cortizas, A., Pontevedra-Pombal, X., Nóvoa-Muñoz, J.C., García-Rodeja, E., 1997. Four thousand years of atmospheric Pb, Cd and Zn deposition recorded by the ombrotrophic peat bog of Penido Vello (Northwestern Spain). Water Air Soil Pollution 100, 387–403.

Martínez-Cortizas, A., Garcia-Rodeja, E., Pontevedra Pombal, X., Nóvoa-Muñoz, J.C., Weiss, D., Cherbulin, A., 2002. Atmospheric Pb deposition in Spain during the last 4600 years recorded by two ombrotrophic peat bogs and implications for the use of peat as archive. Science Total Environment 292, 33–44.

Mighall, T.M., Abrahams, P.W., Grattan, J.P., Hayes, D., Timberlake, S., Forsyth, S., 2002. Geochemical evidence for atmospheric pollution derived from prehistoric copper mining at Copa Hill, Cwmystwyth, mid-Wales, UK. Science of the Total Environment 292, 69–80.

Mighall, T.M., Timberlake, S., Foster, I.D.L., Krupp, E., Singh, S., 2009. Ancient copper and lead pollution records from a raised bog complex in Central Wales, UK. Journal of Archaeological Science 36, 1504–1515.

Mihaljevič, M., Zuna, M., Ettler, V., Šebek, O., Strnad, L., Goliáš, V., 2006. Lead fluxes, isotopic and concentration profiles in a peat deposit near a lead smelter (Pribram, Czech Republic). Science of the Total Environment 372, 334–344.

Monna, F., Lancelot, J., Croudace, I., Cundy, A.B., Lewis, T., 1997. Pb isotopic signature of urban air in France and in UK: implications on Pb pollution sources. Environmental Science and Technology 31, 2277–2286.

Monna, F., Loizeau, J.-L., Thomas, B.A., Guéguen, C., Favarger, P.-Y., 1998. Pb and Sr isotope measurements by inductively coupled plasma–mass spectrometer: efficient time management for precise improvement. Spectrochimica Acta B 59, 1317–1333.

Monna, F., Loizeau, J.-L., Thomas, B., Guéguen, C., Favarger, P.-Y., Losno, R., Dominik, J., 2000. Noise identification and sampling frequency determination for precise isotopic measurements by quadrupole-based inductively coupled plasma mass spectrometry. Analusis 28, 750–757.

Monna, F., Petit, C., Guillaumet, J.-P., Jouffroy-Bapicot, I., Blanchot, C., Dominik, J., Losno, R., Richard, H., Lévêque, J., Chateau, C., 2004a. History and environmental impact of mining activity recorded in a peat-bog (Morvan, France). Environmental Science and Technology 38, 657–673.

Monna, F., Galop, D., Carozza, L., Tual, M., Beyrie, A., Marembert, F., Chateau, C., Dominik, J., Grousset, F.E., 2004b. Environmental impact of early Basque mining and smelting recorded in a high ash minerogenic peat deposit. Science of the Total Environment 327, 197–214.

Monna, F., Poujol, M., Annegarn, H., Losno, R., Coetze, H., Dominik, J., 2006. Origin of atmospheric lead in Johannesburg, South Africa. Atmospheric Environment 40, 6554–6566.

Nriagu, J.O., 1983. Lead and Lead Poisoning in Antiquity. Wiley, New York.

Nriagu, J.O., 1996. A history of global metal pollution. Science 272, 223–224.

Renberg, I., Bindler, R., Brännvall, M.-L., 2001. Using the historical atmospheric lead-deposition record as a chronological marker in sediment deposits in Europe. Holocene 11, 511–516.

Rosman, K.J.R., Chisholm, W., Hong, S.M., Candelone, J.P., Boutron, C.F., 1997. Lead from Carthaginian and Roman Spanish mines isotopically identified in Greenland ice dated from 600 BC to 300 AD. Environmental Science and Technology 31, 3413–3416.

Settle, D., Patterson, C., 1980. Lead in albacore: guide to lead pollutions in Americans. Science 207, 1167–1176.

Shotyk, W., 1996a. Peat bog archives of atmospheric metal deposition: geochemical evaluation of peat profiles, natural variations in metal concentrations, and metal enrichment factors. Environmental Review 4, 149–183.

Shotyk, W., 1996b. Natural and anthropogenic enrichments of As, Cu, Pb, Sb, and Zn in ombrotrophic vs. minerotrophic peat bog profiles, Jura Mountains, Switzerland. Water Air Soil Pollution 90, 375–405.

Shotyk, W., 2002. The chronology of anthropogenic, atmospheric Pb deposition recorded by peat cores in three minerogenic peat deposits from Switzerland. Science of the Total Environment 292, 19–31.

Shotyk, W., Cheburkin, A.K., Appleby, P.G., Fankhauser, A., Kramers, J.D., 1997. Lead in three peat bog profiles, Jura Mountains, Switzerland: enrichment factors, isotopic composition, and chronology of atmospheric deposition. Water Air and Soil Pollution 100, 297–310.

Shotyk, W., Weiss, D., Appleby, P., Cherbukin, A., Frei, R., Gloor, M., Kramer, J., Reese, S., Van der Knaap, W., 1998. History of atmospheric lead deposition since 12, 370 14C yr BP from a peat bog, Jura Mountains, Switzerland. Science 281, 1635–1640.

Shotyk, W., Goodsite, M.E., Roos-Barraclough, F., Frei, R., Heinemeier, J., Asmund, G., Lohse, C., Hansen, T.S., 2003. Anthropogenic contributions to atmospheric Hg, Pb and As accumulation recorded by peat cores from southern Greenland and Denmark dated using the 14C "bomb pulse curve". Geochimica Cosmochimica Acta 67, 3991–4011.

Vile, M.A., Wieder, R.K., Novak, M., 1999. Mobility of Pb in Sphagnum-derived peat. Biogeochemistry 45, 35–52.

Wedepohl, K.H., 1995. The composition of the continental crust. Geochimica et Cosmochimica Acta 59, 1217–1232.

Weiss, D., Shotyk, W., Appleby, P.G., Cheburkin, A.K., Kramers, J.D., 1999. Atmospheric Pb deposition since the Industrial Revolution recorded by five Swiss peat profiles: enrichment factors, fluxes, isotopic composition, and sources. Environmental Science and Technology 33, 1340–1352.

Weiss, D., Shotyk, W., Boyle, E.A., Kramers, J.D., Appleby, P.G., Cheburkin, A.K., 2002. Comparative study of the temporal evolution of atmospheric lead deposition in Scotland and eastern Canada using blanket peat bogs. Science Total Environment 292, 7–18.